

# Motion of a Cell Wall Polysaccharide Observed by Atomic Force Microscopy

A. Patrick Gunning, Alan R. Mackie, Andrew R. Kirby, Paul Kroon, Gary Williamson, and Victor J. Morris\*

*Institute of Food Research, Norwich Research Park, Colney, Norwich NR4 7UA, U.K.*

*Received February 23, 2000; Revised Manuscript Received May 4, 2000*

**ABSTRACT:** A water-soluble wheat pentosan polysaccharide has been observed in motion by atomic force microscopy (AFM). The motion occurred under aqueous buffer solution and has been attributed to the desorption and readsorption of segments of the molecule from the mica substrate on to which it had been physisorbed. The three classically described states postulated to be involved in polymer adsorption/desorption, namely loops, trains and tails were confirmed by direct observation. These observations validate long held, but largely untested, beliefs about the nature of the adsorption/desorption of polymer chains to surfaces.

## Introduction

Adsorption of polymers to surfaces is a widely studied phenomena which has bearing on many different disciplines. These range from industrial concerns, such as the fouling of surfaces in processing equipment on one hand,<sup>1</sup> to more fundamental questions in biology on the other, such as the role that pattern recognition is proposed to play during site directed binding of heterogeneous polymers in the biosynthesis of complex natural structures.<sup>2</sup> Polymer adsorption to surfaces has been modeled extensively (for a review see Fleer and co-workers<sup>3</sup>). More recently, modeling of polymer adsorption to surfaces has been extended to the study of site specific adsorption.<sup>4,5</sup> The complexity of such modeling has meant that, until relatively recently, these studies have tended to be concerned only with homogeneous polymers or diblock copolymers.<sup>5</sup> However, very recently, modeling has been extended to heteropolymers adsorbing to heterogeneous surfaces, and the effect that pattern matching may play in directing the adsorption.<sup>6,7</sup> This is closer to the situation one might expect to find in real biological systems, where either nonspecific or specific adsorption of protein or polysaccharide molecules to particular surfaces may arise. Theoretical models are generally difficult to verify through conventional experimental observations since most techniques tend to measure the average properties of such systems over the entire population of the sample and cannot therefore visualize events for individual molecular species. This situation has changed recently with the advent of scanning probe microscopy, which allows dynamic molecular processes to be visualized directly and at very high resolution.<sup>8</sup>

The present study describes the experimental observation, by atomic force microscopy, of the motion of a plant cell wall arabinoxylan polysaccharide (a water-soluble wheat pentosan) which has been adsorbed to a mica substrate. The molecular motion is attributed to desorption/adsorption of segments of the polysaccharide molecule.

## Experimental Section

Arabinoxylan was extracted from wheat flour using previously described methods.<sup>9</sup> The freeze-dried polymer was dis-

solved in distilled water to a concentration of  $2 \mu\text{g mL}^{-1}$  by vortexing at room temperature ( $21^\circ\text{C}$ ). A  $2 \mu\text{L}$  drop of the solution was deposited onto freshly cleaved mica and allowed to dry in air at room temperature. The mica was then inserted into the liquid cell of the AFM and the buffer solution added to the cell.

Atomic force microscopy was carried out under a solution of 10 mM HEPES buffer, which contained 2 mM  $\text{ZnCl}_2$  (pH 7.4), using an ECS AFM (Cambridge, England) operating in the "tapping mode" using 100  $\mu\text{m}$  long oxide sharpened Nanoprobe levers (NP-S, Santa Barbara) with a quoted force constant of  $k = 0.38 \text{ N m}^{-1}$ . The natural (undriven) resonance behavior was measured in air by monitoring the noise signal of the lever with a spectrum analyzer. This gave peaks at 33 and 42 kHz. Under liquid, a large number of resonant peaks were observed between 29 and 43 kHz. In this study the resonance at 36.8 kHz produced the most stable operating conditions. In the instrumental setup used for the present studies, the cantilever on which the AFM tip is mounted is oscillated just below resonance (36.8 kHz) by applying a small sinusoidal drive signal to the  $Z$  axis of the piezoelectric scanner. The liquid in the cell, which sits on top of the scanner, transmits this oscillation to the cantilever by viscous coupling. The drive frequency used was 36.4 kHz, and the drive voltage 50 mV; this produced an oscillation amplitude of the cantilever itself of approximately 12 nm. In the so-called "tapping modes" of imaging the AFM tip is in transient contact with the sample surface. In fact the tip touches the surface only at the end of each cycle, producing dramatically less shear force between the tip and the surface than the conventional contact mode imaging process,<sup>10,11</sup> which is an important consideration in this study. The imaging force was minimized by operating at a set point at which the tip just tracked the surface in a stable manner. This corresponded to about 5% damping of the amplitude of oscillation of the tip cantilever assembly.

Image analysis was carried out using ImagePro (Media Cybernetics Inc.). To produce an animated sequence of the AFM images, from which tracking of the polysaccharide could be carried out, the frames were registered to eliminate instrumental drift. The first AFM image in the sequence was used as the reference image, and registry was effected by overlaying subsequent images, after reducing their opacity, such that the background image could be seen "through" the overlaid image. The top image was then moved around until the "best fit" of the backgrounds between the two images was achieved. In fact the background pattern of small blobs of "debris" in the images was remarkably stable for all of the images, making this task quite straightforward. When a true fit was achieved the background appeared to jump into focus.

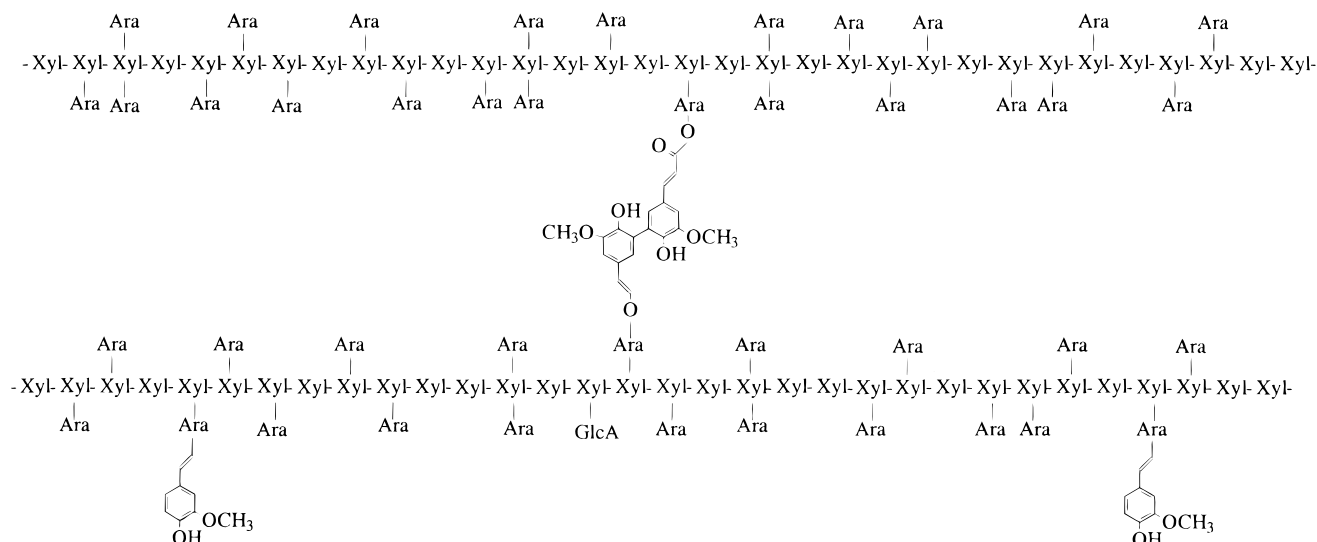


**Figure 1.** Probable chemical structure of a water-soluble wheat arabinoxylan. Chemical and enzymatic degradation methods have indicated that these polymers consist of a backbone of  $\beta$ -1,4-linked D-xylose (Xyl) residues which are substituted mainly with single L-arabinofuranose (Ara) substituents which can be  $\alpha$ -1,2- or  $\alpha$ -1,3-linked.<sup>17</sup> A portion of the arabinose side chains may be further substituted with ferulic acid or dehydromers of ferulic acid through a 1,5-ester linkage.<sup>18</sup> It has been demonstrated that ferulic acid dehydromers cross-link arabinoxylans.<sup>19,20</sup> A small number of  $\alpha$ -1,2-linked glucopyranosyluronic acid (GlcA) substituents may be present, imparting an overall negative charge.

A probability map of molecular position over the entire sequence was also generated using ImagePro. First the registered images were thresholded to produce an image mask which contained predominantly the arabinoxylan plus a few of the brighter background features which occupied the same or higher gray levels in the images. Each image mask was converted into a binary image (i.e., black and white) and stored as an 8 bit grayscale image. Finally, all of the 8 bit binary mask images were added together onto a blank 16 bit grayscale image (to avoid tonal saturation) to produce one final image where the gray level at any given point represented the probability of adsorption of part of the arabinoxylan molecule. This was then converted into a false color image to aid viewing.

## Results

The polymer examined in this study was a cell wall polysaccharide: a water-soluble wheat pentosan, composed mainly of a xylose backbone with arabinose side chains, and termed an arabinoxylan (Figure 1). The backbone of the arabinoxylan is composed of a  $\beta$ -1,4 linked xylose, which is substituted with irregularly placed side chains of  $\alpha$ -1,3 and  $\alpha$ -1,2 linked single arabinose groups along its length. The arabinose side chains are themselves occasionally substituted with ferulic acid groups, which can dimerize and form cross-links between two arabinoxylan polymer molecules, as illustrated in Figure 1. The polymer contains small amounts of glucuronic acid which give a net negative charge.

Figure 2 shows a typical AFM image of arabinoxylans which have been deposited onto mica, air-dried to promote adhesion, and then imaged under aqueous buffer. The image illustrates the two most common appearances for the arabinoxylans seen in the present AFM study, namely linear and entangled "shoe-lace" shaped structures. In both cases the arabinoxylans appear to be extended semiflexible chains. X-ray diffraction studies suggest that the wheat pentosans should adopt a 3-fold helical structure.<sup>12</sup> The extended nature of the structures shown in Figure 2 suggest that they are in the helical form. Clearly some of the polymers are linear structures. For the more complex

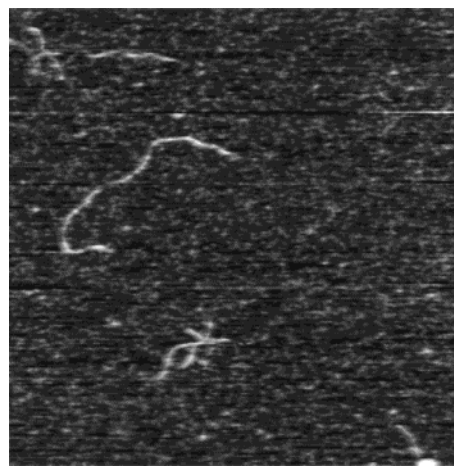


**Figure 2.** Typical AFM images of arabinoxylans adsorbed onto mica, imaged under aqueous buffer, illustrating different shapes adopted by the polysaccharides. Scan size: 1000 nm  $\times$  1000 nm.

images it is not easy to draw conclusions about molecular shape. The structures observed could be branched molecules, aggregates or structures formed by the molecules folding back on themselves when they adsorb. As will be seen later, this is further complicated by the fact that the arrangement of segments of the molecule may change during scanning, and the final image may be a superposition of more than one arrangement on the mica surface.

Figure 3, parts a–f, shows a consecutive series of AFM images of an arabinoxylan in the "shoe-lace" shape on the mica substrate. These images were recorded under buffer solution in a separate experiment to that presented in Figure 2. The time interval between each image was approximately 1 min. Comparison of successive images in the sequence in Figure 3 reveal that the arabinoxylan undergoes several alterations to its shape on the substrate, suggesting that it was moving between, and probably during, the imaging process. To allow measurement of this movement, instrumental

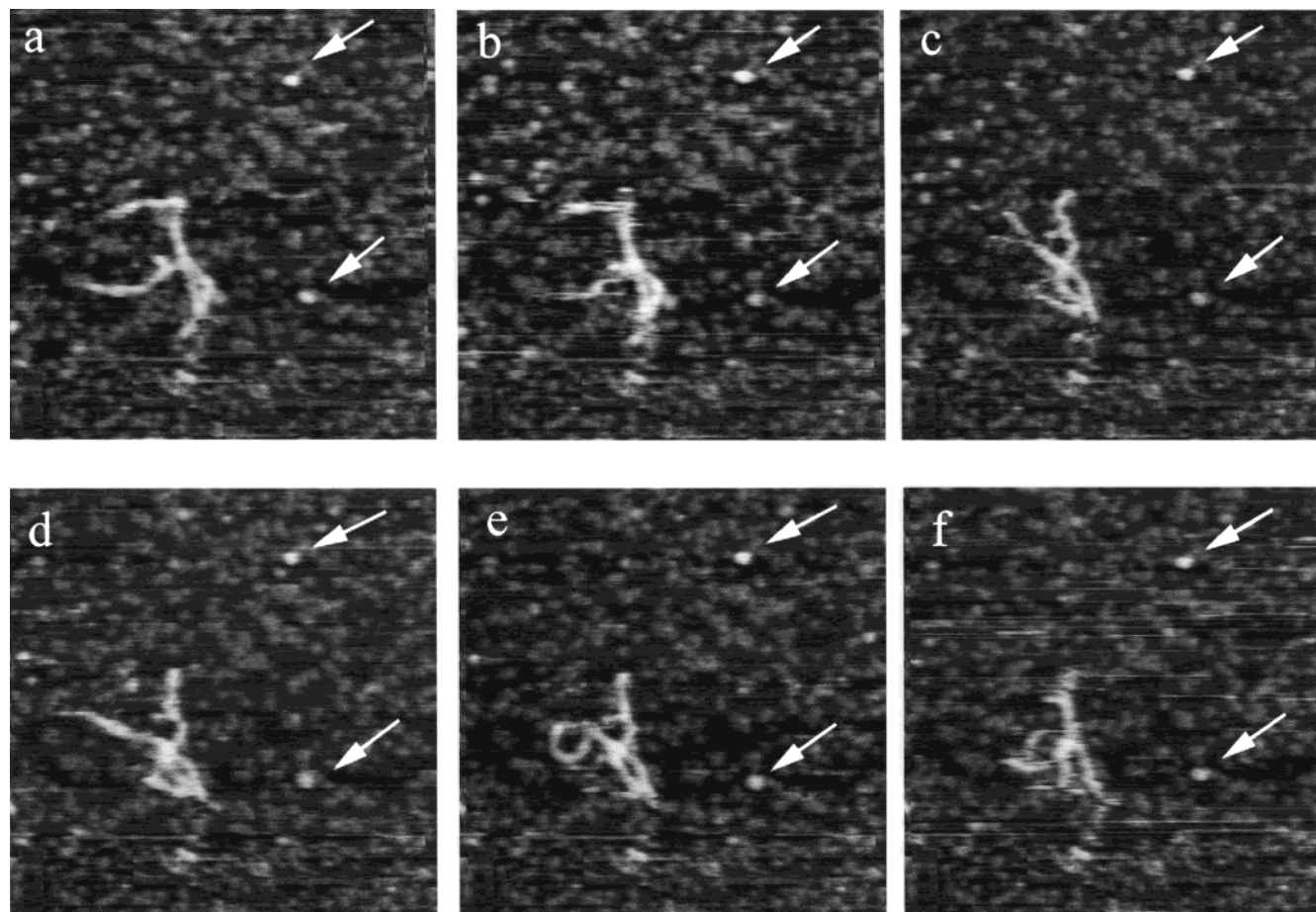


**Figure 3.** Consecutive sequence of AFM images of an arabinosyl adsorbed onto mica and imaged under aqueous buffer, illustrating apparent movement of the polysaccharide as indicated by changes in shape. The arrows indicate molecular debris on the mica which shows no movement during scanning. Scan size: 600 nm  $\times$  600 nm.

drift was removed by registering the images, as described in the Experimental Section. To demonstrate the validity of this process we have arrowed two prominent features on the mica substrate in Figure 3 which serve as useful static references for the eye. There are many such background features or "debris" which are probably due to impurities in the buffer solution that adsorb preferentially to certain regions on the mica. While undesirable in terms of image contrast, this background contamination is useful for the purposes of image registration, and also in confirming that the motion of the arabinosyl seen in Figure 3 is not simply due to instrumental drift. Careful examination of virtually all of the background features reveals that they are static throughout the sequence, in stark contrast to the arabinosyl which clearly changes shape. The "motion" of the polysaccharide is currently displayed as a molecular movie (<http://www.ifr.bbsrc.ac.uk/FQM/SPM/>) and the animation file is deposited as Supporting Information. Having verified that the motion is real, it is then necessary to explain how this motion occurs.

There are two obvious possible mechanisms: reptation of the polysaccharide on the mica surface, or apparent changes in shape due to consecutive desorption and readsorption of segments of the polysaccharide chain.

The first mechanism could simply be reptation of the arabinosyl across the mica surface, either spontaneously or induced by interactions with the AFM tip. This first mechanism is considered to be unlikely for the

following reasons. This type of apparent motion of arabinosyls was only ever seen when the imaging was done in aqueous buffer. If imaging was carried out under a precipitant, such as butanol, no motion was observed. Since the molecule was physisorbed to the mica substrate in the same way in both cases (air-drying), this suggests that reptation is an unlikely candidate for explaining the changes in shape. Similarly, reptation induced by dragging or "shovelling" of the molecule across the mica surface by interactions with the AFM tip might also reasonably be ruled out, since this should be equally likely to occur irrespective of the liquid under which the sample is imaged. The observation of molecular debris, which is not swept from the scan by the probe, also supports the assertion that tip interactions with the sample are likely to be minimal. The AFM images obtained in this study were carried out in "tapping mode" in liquid, which should virtually eliminate lateral force interactions between the AFM tip and surface, reducing the likelihood of the sample being pushed or dragged by the tip.

The second mechanism by which motion of the arabinosyl may occur is via partial desorption of the polysaccharide chains from the mica, into the bulk solution, followed by readsorption back onto the mica surface in a different orientation. This would be observed as a change in shape of the polysaccharide. This second version of events would be described by the classically accepted models for polymer adsorption/desorption to surfaces, which define three different



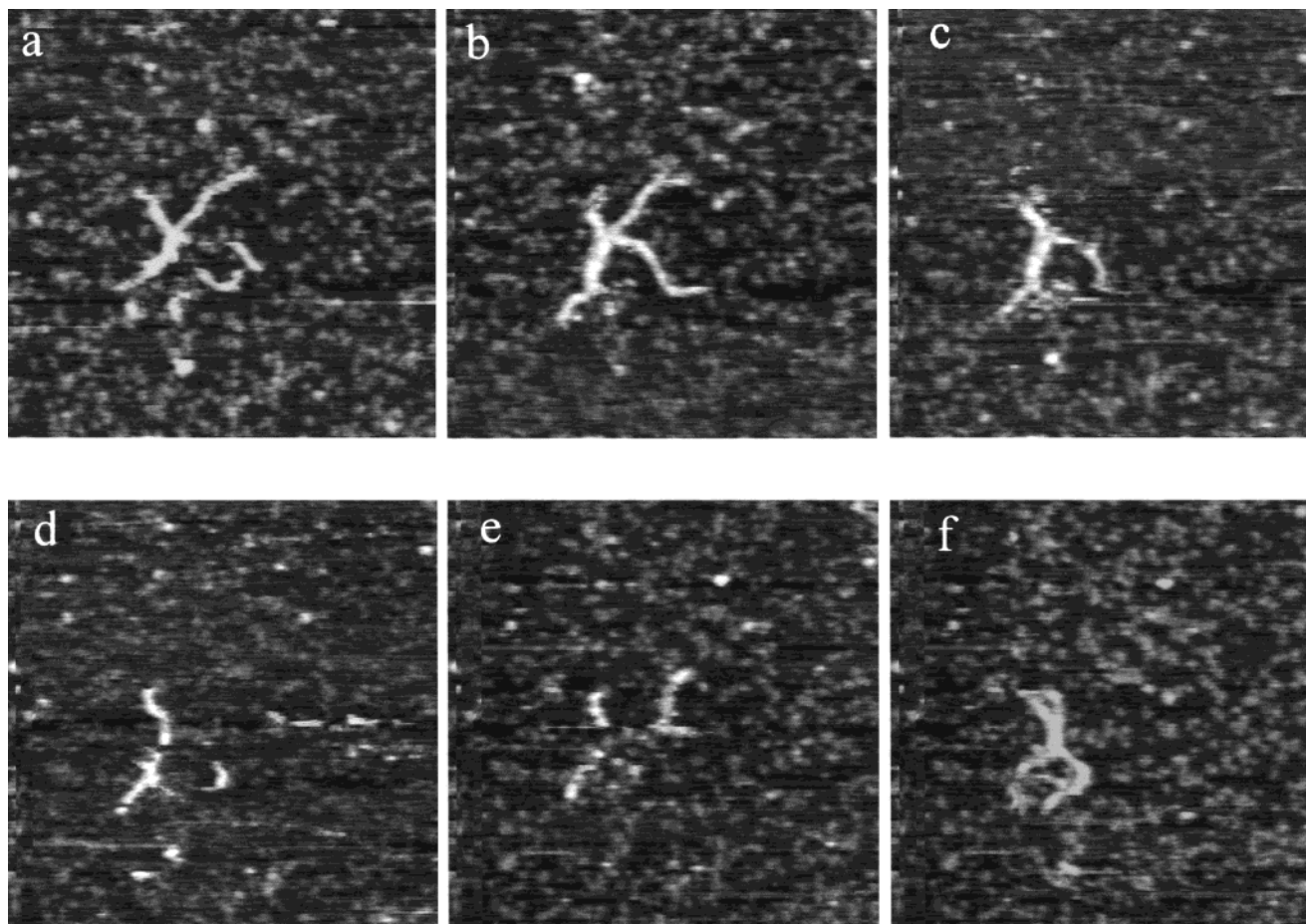


**Figure 4.** Consecutive sequence of AFM images of an arabinoxylan polysaccharide adsorbed onto mica and imaged under aqueous buffer, illustrating "loops, trains, and tails". Scan size: 600 nm  $\times$  600 nm.

possible states that segments of adsorbed polymers can adopt, namely "loops", "trains", and "tails".<sup>3,13</sup> Trains are defined as regions of the polymer chains which are bound to the surface, while loops are unbound regions of the chain, which are therefore in solution but, which connect two such bound trains. Finally, tails are non-adsorbed or free chain ends. This loop, train, and tail mechanism seems to be the most likely explanation for the apparent motion of the arabinoxylans for the following reasons. The arabinoxylan molecules are water soluble, and hence the concentration of molecules adhering to the mica under aqueous buffers should be low. The air-drying step will initially enhance this concentration. After immersion of the sample in buffer the enhanced surface concentration should promote desorption and struggles of the molecules to enter the bulk phase could be perceived as molecular motion. It is envisaged that segments of the polysaccharides enter the bulk phase, and then subsequently readsorb in a different position, causing a change in shape of the arabinoxylan. This scenario is consistent with the previously mentioned observations that arabinoxylan molecules air-dried onto mica, but imaged under the precipitant butanol, have never shown any evidence of such motion. This would be expected because there would not be the same drive to desorption expected under a precipitant for the polysaccharide. In addition to the inferred evidence described above, some of the sequences of AFM images obtained provide direct experimental evidence for the existence of loops, trains, and tails. Examples of such images are presented in

Figure 4. This figure shows another consecutive series of AFM images of the arabinoxylans on mica under aqueous buffer. In Figure 4a the polysaccharide appears to have a break on the lower right segment of the chain. Figure 4b, which was obtained 1 min later, reveals that the break has apparently "healed" and the segment has altered its position slightly. In Figure 4c the upper right segment appears to have completely desorbed. In the next two scans in the sequence (Figure 4, parts d and e) the polysaccharide shows many breaks which again reappear in the final scan in this part of the sequence, but now the apparently intact polymer has a radically altered shape (Figure 4f). The reappearance of the apparently "broken" segments (Figure 4, parts d and e) which can now be observed in Figure 4f suggest that they were in fact loops which, because they were in solution and in motion, could not be imaged by the AFM tip. Following this argument, the disappearance of an entire segment of the polysaccharide chain, as seen in Figure 4c, suggests that this segment has desorbed to become a so-called tail. Thus, all three possible states described in Jenkel and Rumbachs' model of polymer adsorption<sup>13</sup> can be identified in the AFM images of arabinoxylans presented here in Figure 4.

The AFM collects images by raster scanning the sample. If the start time of each scan is known then it is possible to follow the occupancy of each pixel in the image as a function of time. This type of information could be of use in testing theoretical models of polymer adsorption/desorption. Because it takes a finite time to acquire a scanned image, then if parts of the molecule

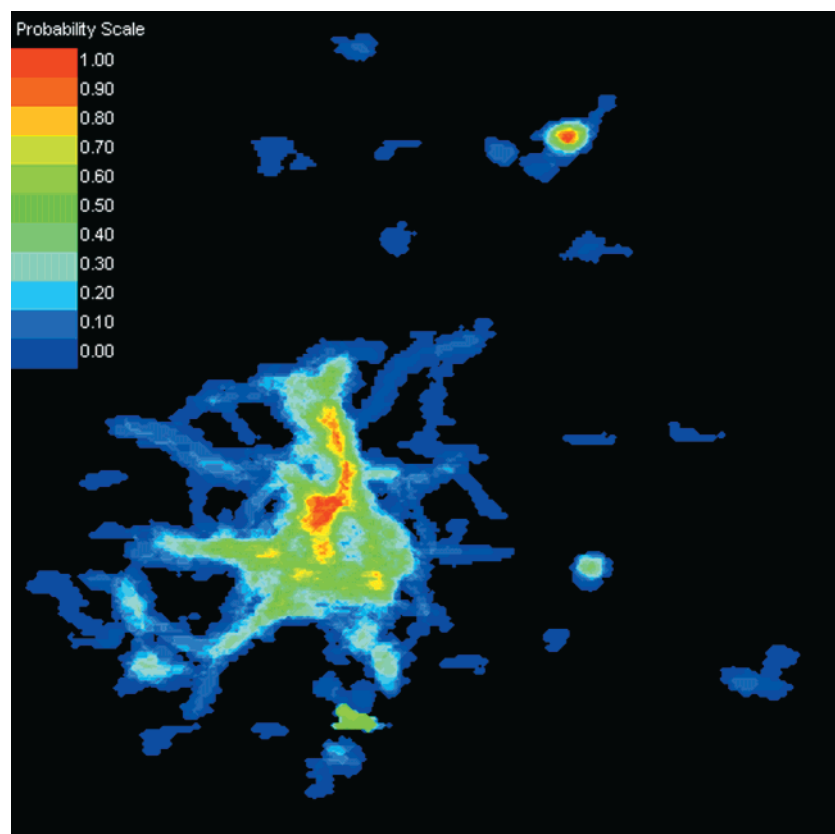


**Figure 5.** False color image representing the probability of finding a segment of the arabinosylian bound to the mica surface. The image was generated by summing over a sequence of 40 scans and averaging the data. A probability of 1 represents 100% occupancy of the location. Scan size: 600 nm  $\times$  600 nm.

move during the scan, the final image may include the same segment of the molecule in one or more positions. A true sequence of images could be generated by interpolating the time dependent data at each pixel, and constructing new "images" at fixed times. Such images would provide a better representation of the true shape of the molecule. The motion of the arabinosylian can also be quantified by generating an adsorption probability map: this involves adding the total number of images after alignment. Such a time-averaged structure is shown in Figure 5. The colors in the image represent the likelihood of finding a part of the polysaccharide bound to the mica at any given time, summed throughout the whole sequence of images. The colors in the map have been assigned a level ranging from blue at the low probability end to red at the high probability end. Examination of Figure 5 reveals that the distribution of color, and thus adsorption probability, was not entirely random, with the central regions of the arabinosylian showing a stronger affinity for the mica surface. This suggests that there was some form of preferential interaction between these central regions of the molecule and the mica surface. Such attachment may indicate some degree of heterogeneity of the molecular structure of the arabinosylian molecules but, more likely, reflects the fact that motion of molecular segments becomes easier as one approaches the "free ends" of the molecular chains. It should be noted that over the duration of the sequence only a few segments of the polysaccharide, close to what appears to be the center of the molecule, showed 100% adsorption to the mica substrate.

There are reports of observation of the molecular motion of DNA chains by AFM. The DNA was adsorbed

to mica and then imaged under aqueous solution.<sup>14</sup> Furthermore, "apparent breakages" of DNA chains, which "rehealed" in subsequent scans, have also been observed in AFM studies of the transcription of DNA by an RNA polymerase.<sup>15</sup> In these studies the enzymes were adsorbed to the mica and the DNA bound to the enzyme. In the present studies polysaccharides adsorbed to mica were observed in buffered conditions over extended periods of time. The fact that segments of the molecules entered the bulk phase during this period suggests that it may be possible to observe enzyme binding and enzymatic breakdown of polysaccharides in real time. Preliminary studies of enzymatic synthesis<sup>14</sup> and breakdown<sup>16</sup> have been reported for DNA and indicate that molecular motion is an important requirement for reactions to occur.

**Acknowledgment.** Maria Teresa Garcia Conesa is thanked for isolation of the arabinosylian sample used in this study. Dr Andrew Pinder is thanked for help with image processing and animation. The BBSRC is thanked for funding this research through core funding and a ROPA grant (9708918) to the Institute.

**Supporting Information Available:** The animation sequence described in the text is available free of charge via the Internet at <http://pubs.acs.org>.

## References and Notes

- (1) Sheikholeslami, R. *Environ. Prog.* **1999**, *18*, 113–122.
- (2) Alberts, B.; Bray, D.; Lewis, J.; Raff, M.; Roberts, K.; Watson, J. D. *Molecular Biology of the Cell*; Garland: New York, 1994.
- (3) Fleer, G. J.; Cohen Stuart, M. A.; Scheutjens, J. M. H. M.; Cosgrove, T.; Vincent, B. *Polymers at Interfaces*; Chapman and Hall: London, 1993.

- (4) Muthukumar, M. *J. Phys. Chem.* **1995**, *103*, 4723–4731.
- (5) Chakraborty, A. K.; Tirrell, M. *MRS Bull.* **1996**, *21*, 28–32.
- (6) Chakraborty, A. K.; Bratko, D. *J. Chem. Phys.* **1998**, *108*, 1676–1682.
- (7) Golumbskie, A. J.; Pande, V. S.; Chakraborty, A. K. *Proc. Natl. Acad. Sci. U.S.A.* **1999**, *96*, 11707–11712.
- (8) Kasas, S.; Thomson, N. H.; Smith, B. L.; Hansma, H. G.; Zhu, X.; Guthold, M.; Bustamante, C.; Kool, E. T.; Kashlev, M.; Hansma, P. K. *Biochemistry* **1997**, *36*, 461–468.
- (9) Faurot, A. L.; Saulnier, L.; Berot, S.; Popineau, Y.; Petit, M. D.; Rouau, X.; Thibault, J. F. *Food Sci., Technol. (Leben. Wiss., Technol.)* **1995**, *28*, 436–441.
- (10) Hansma, P. K.; Cleveland, J. P.; Radmacher, M.; Walters, D. A.; Hillner, P. E.; Bezanilla, M.; Fritz, M.; Vie, D.; Hansma, H. G.; Prater, C. B.; Massie, J.; Fukunaga, L.; Gurley, J.; Elings, V. *Appl. Phys. Lett.* **1994**, *64*, 1738–1740.
- (11) Putman, C. A. J.; van der Werf, K. O.; de Grooth, B. G.; van Hulst, N. F.; Greve, J. *Appl. Phys. Lett.* **1994**, *64*, 2454–2456.
- (12) Atkins, E. D. T. *Xylans and Xylanases*; Elsevier Science: New York, 1992; pp 39–50.
- (13) Jenkel, E.; Rumbach, B. *Z. Elektrochem.* **1951**, *55*, 612–618.
- (14) Argaman, M.; Golan, R.; Thomson, N. H.; Hansma, H. G. *Nucleic Acids Res.* **1997**, *25*, 4379–4384.
- (15) Hansma, H. G.; Laney, D. E.; Bezanilla, M.; Sinsheimer, R. L.; Hansma, P. K. *Biophys. J.* **1995**, *68*, 1672–1677.
- (16) Bezanilla, M.; Drake, B.; Nudler, E.; Kashlev, M.; Hansma, P. K.; Hansma, H. G. *Biophys. J.* **1994**, *67*, 2454–2459.
- (17) Aspinall, G. O. *The Biochemistry of Plants*; Academic Press: London, 1980; Vol. 3, pp 473–500.
- (18) Ishii, T. *Plant Sci.* **1997**, *127*, 111–127.
- (19) Ishii, T. *Carbohydr. Res.* **1991**, *219*, 15–22.
- (20) Saulnier, L.; Crépeau, M.-J.; Lahaye, M.; Thibault, J.-F.; Garcia-Conesa, M. T.; Kroon, P. A.; Williamson, G. *Carbohydr. Res.* **1999**, *320*, 82–92.

MA000331W